Special Issue Published in International Journal of Trend in Research and Development (IJTRD), ISSN: 2394-9333, www.ijtrd.com

# In-Situ Observation of Growth Morphologies in Organic Peritectics

Johann P. Mogeritsch[a], Andreas Ludwig[a]
[a]Department of Metallurgy, Chair for Simulation and Modelling Metallurgical Processes, Montanuniversitaet Leoben, Austria

***Abstract***: Directional solidification experiments were performed with the binary transparent organic model system TRIS-NPG to investigate peritectic solidification close to the limit of constitution under cooling. The experiments were carried out as in-situ observation in a vertical micro Bridgman-furnace. Since the primary and the peritectic phases do not differ optically, only changes at the phase boundaries are visible. In this paper, we report on observed solidification morphologies. Growth of the peritectic phase in the interstitial liquidoccurred under conditions in which both phases solidify in a cellular or dendritic manner. Peritectic layered structures were detectedclose to the critical velocity,at which both phases solidify in a planar manner. For a planar solidification front, the formation of the peritectic phase in the form of roundish inclusions was observed,whereby theseinclusions have originate at the solid/liquid interface.

***Keywords:*** *Organic Model System, Peritectic Solidification Structures, Bridgman-Furnace,*

## I. INTRODUCTION

The evolution of humanity is closely linked to the ability to process metals and make alloys. Copper is one of the few metals that can occur in nature in a directly usable metallic form and has been used by humansfor at least 10.000 years. It was the first metal to be purposefully alloyed with another metal, tin, to create bronze around 3500 BC. This alloy exhibits a peritectic equilibrium which is also found in many other very common alloys today like steel, brass, high temperature conductors or rare earth permanent magnets. In peritectic alloys, the liquid [L], the primary solid [α] phase, and the peritectic [β] phase are in equilibrium at the peritectic temperature, $T_p$. Typical peritectic systems for metals have a temperature dependent solute solubility in the peritectic phase, where as rare earth permanent magnet alloys and ceramic super conductors commonly display either a very narrow or no solubility region.

Depending on the process conditions, a dendritic, cellular or planar interface can be obtained. Since the kinetics and the rate of diffusion in the solid phase is slow compared to the liquid phase, this determines the time it takes to reach an equilibrium. Therefore, in most cases the system is in a thermodynamic imbalance. As a consequence, under dendritic/cellular growth conditions, the peritectic phase can solidify directly from the interstitial lliquid instead of forming by transition. In the case of planar growth it is possible that neither the primary nor the peritectic phase can reach a growth state that corresponds to thermodynamic equilibrium. As consequence alternative primary and peritectic layers perpendicular to the growth direction form as shown by Boettinger [1]. Trivedi [2] provides a theoretical model to explain such banded structures under purely diffusion conditions. Furthermore, it has become obvious from investigations of directional solidified peritectic alloys like Zn–Ag [3], Sn–Cd [1, 4-6], Cu-Sn [7], Pb–Bi [8-11], Zn–Cu [12, 13], Sn–Sb [14], Ti–Al [15], Fe–Ni [16-20], Ni–Al [21], and Nd–Fe–B [22] that peritectic systems show a variety of complex microstructures. Close or below the limit of constitutional undercooling, where both phases solidify in a planar fashion, isothermal peritectic coupled growth (PCG), cellular peritectic coupled growth, discrete bands, island bands, and oscillatory tree-like structures were found. It is especially the observation of two-phase competitive growth, either coupled or banded, which has drawn attention to using transparent, organic components from TRIS and NPG [23] as model systems for in-situ observation of peritectic layered solidification morphologies [24-37].

## II. PROBLEM IDENTIFICATION AND BASIC PRINCIPLE

In the present work, we analyze solidification morphologies for dendritic/cellular and planar growth conditions by using the binary organic substances TRIS-NPG as a model system for peritectic metallic solidification. In particular, we concentrate on the occurrence of the peritectic phase and the conditions necessary for peritectic couple growth.

## III. METHODOLOGY

Directional solidification experiments were carried out by using the Bridgman technique. The cooling and heating zone consisted of brass plates with a milled guide for a rectangular glass sample, enclosed by a ceramic thermal shelter. Samples were pulled vertically at a constant,PC-controlled velocity through the temperature gradient ($G_T$ = 7.2·10$^{-3}$ K/m) within the adiabatic zone. The sample was illuminated through the adiabatic zone to observe the dynamics of the solid/liquid (s/l) interface and the solidification morphology with a light transmission microscope. Images were continuously recorded with a CCD camera for a subsequent evaluation (see Fig. 1).

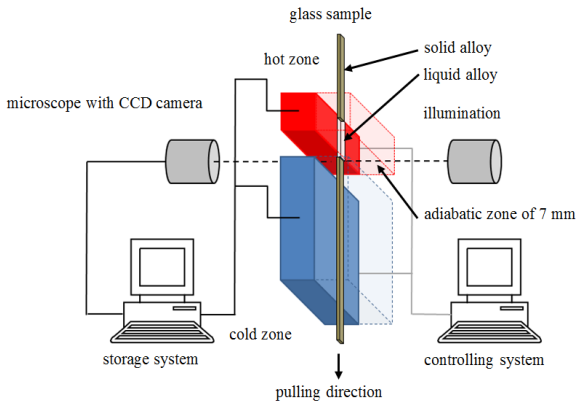


Fig. 1:Sketch of the Bridgman furnace.

The model system consists of the two organic substances: TRIS and NPG. Details of the peritectic region are shown in Fig. 2. The peritectic plateau is divided by the peritectic concentration $C_p$into the hypo- ($C_\alpha \le x \le C_p$) and the hyper-

peritectic ($C_p \leq x \leq C_L$) region. NPG, with a purity of 99%, and TRIS with 99.9$^+$ % were used as delivered and alloys within the peritectic concentration ($0.47 \leq x \leq 0.54$ mol fraction NPG) were prepared within a glove box under an argon atmosphere.

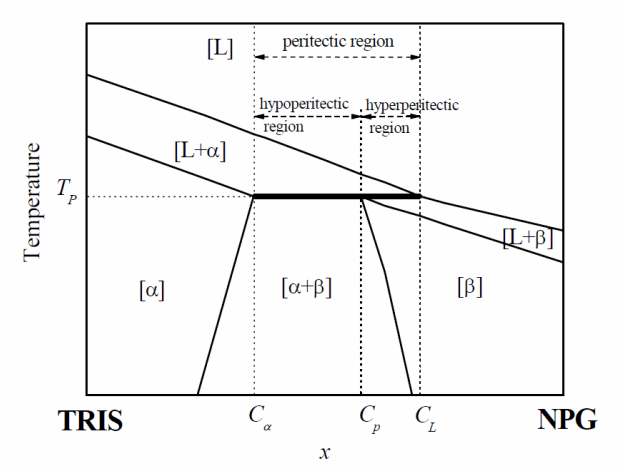


Fig. 2: Peritectic plateau of the model system TRIS–NPG[23].

We prepared the compound by mixing in the solid state and homogenized it by melting and cooling, respectively. The obtained compound was ground to a powder to make the sample. More details are given in [24, 26].

The sample was manufactured by capillary force filling the rectangular quartz tubes (100 x 2000 µm$^2$ cross sectional area, 100 µm glass wall thickness) with the organic compound and sealed with a UV-hardening glue. The glass sample was placed into the furnace remaining stationary for 1 hour to reach a state of thermal equilibrium. The sample was pulled through the furnace at a constant rate.

Compounds close to the peritectic concentration were investigated by using a temperature gradient - pulling velocity ratio in the range of $3.2{\cdot}10^{10} \leq G_T/V_p \leq 5.65{\cdot}10^{10}$ s·K/m$^2$. The results presented here were taken from two experiments for a hypo-peritectic concentration with $x$ = 0.49 ± 0.01 and one experiment for a hyper-peritectic compound with $x$ = 0.53 ± 0.01 mol fraction NPG.

## IV. RESULTS

### *A. Primary and peritectic solidification*

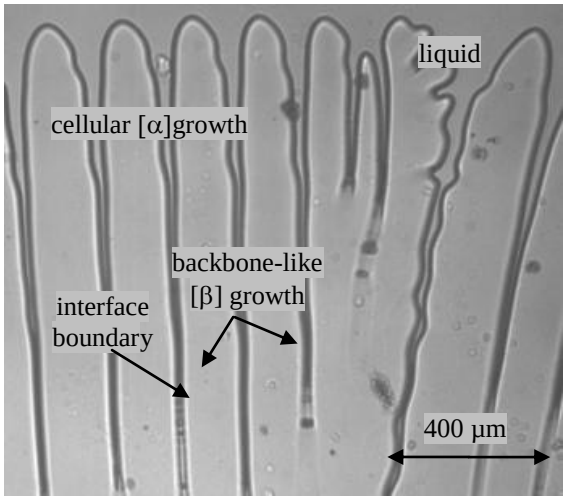


Fig. 3: Cellular solidification morphology with interstitial peritectic growth. ($x$ = 0.49, $G_T/V_p = 3.2{\cdot}10^{10}$ s·K/m$^2$)

Above the so-called constitutional undercooling velocity, the solidification morphology in the hypo-peritectic region shows a cellular growth for the primary [α] phase and within the interstitial liquidan unsteady backbone-like growth of the peritectic [β] phase, asshown in Fig. 3. The new created interface boundaries between the two different solidification events are clearly distinguishable. The cells grow continuously, whereas the backbone-like growing phase in the interstitial liquid solidify discontinuously in an irregular manner as described later.

### *B. Layered solidification morphology*

In the same concentration range, but for process conditions closer to the critical velocity, the s/l interface shows initially a planar appearance.In the further course of the solidification experiment, small perturbations occurand destabilize the planar s/l interface. Simultaneously, a new phasenucleates in the region close to the right side wallfrom where it grows laterally toward the center of the sample (Fig. 4). In such a way, a band perpendicular to the front forms.

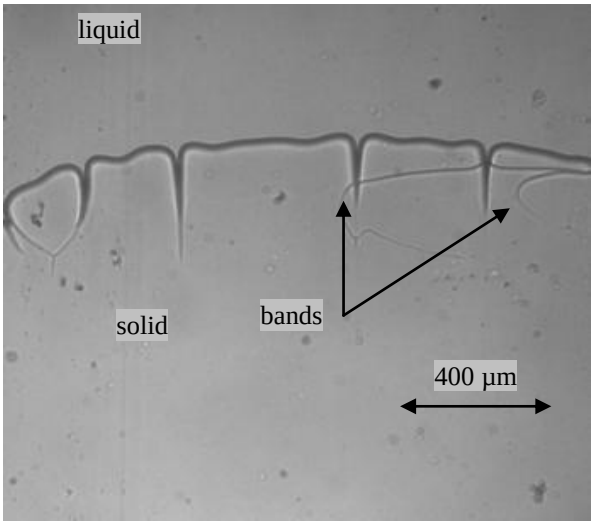


Fig. 4: Formation of a layered solidificationstructure.

($x$ = 0.49, $G_T/V_p = 3.8{\cdot}10^{10}$ s·K/m$^2$)

Such bands grow preferable at the fore- and background such that it engulfs the initial phase except at the top where a competitive growth between the two phases occurs as discussed in the next section. After some period of time the competitive coupled peritectic growth terminates and the initial phase starts again to be the preferred phase by now growing with deep cells.

### *C. [β] phase inclusions*

For the hyper-peritectic concentration $x$ = 0.53, we found small spherical [β] phase inclusions that form right at or at some distance below the α/l interface (Fig. 5).

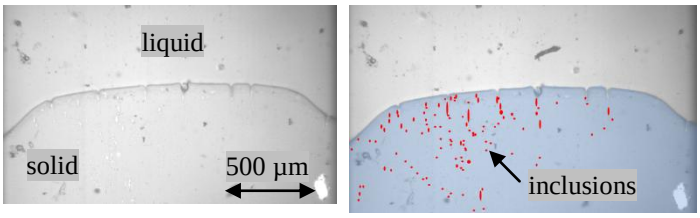


(a) (b)

Fig. 5: [β] phase inclusions (red) within the [α] phase matrix (blue).($x$ = 0.53, $G_T/V_p = 5.6{\cdot}10^{10}$s·K/m$^2$)

While forming these inclusion, the α/l interface passes through

morphological instabilities. No further interaction between die primary [α] phase and the peritectic [β] phase inclusions was observed.

## V. DISCUSSION

### *A. Interstitial peritectic solidification*

According to the TRIS-NPG phase diagram and the selected concentration $x$ = 0.49, the initial phase is identified as the primary [α] phase. For this alloy and slightly above at the peritectic temperature, $T_p$,64% [α] phase is in equilibrium with 36% liquid. Note that as $\rho_l \approx \rho_\alpha \approx \rho_\beta$, mass and volume fraction are comparable. Just below $T_p$, around 50% [α] phase is in equilibrium with around 50% [β] phase. Thus according to thermodynamics, at $T_p$, the amount of [α] has to decrease from 64% to 50% that's by 22%, which means that a large amount of [α] must transform into [β]. So, theoretically the [β] phase forms from both the melt and the [α] phase. None of these thermodynamic arguments were found to be valid in the present case. That indicates that for the selected process conditions the system is far from being in thermodynamic equilibrium.

Careful observation of the interstitial liquid shows that the remaining liquid solidifies in a backbone-like manner but discontinuously in form of segments rather than continuously (Fig. 6).

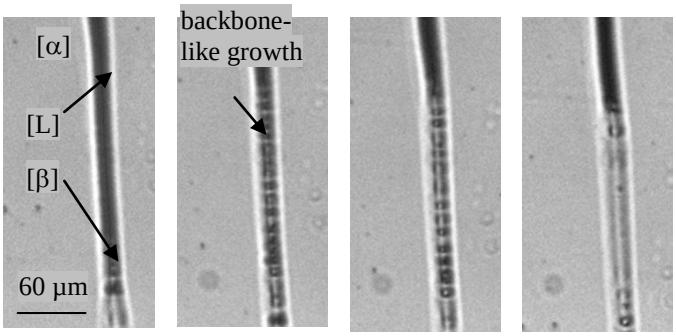


Fig. 6: Backbone-like growth of the peritectic phase in the interstitialliquid for $x$ = 0.49.

Initially, there is no growth within the interstitial liquid until quite abrupt the peritectic [β] phase occurs as segment –up to 100 microns grow within a few seconds. It appearance resemble a typical backbone segment with again interstitial liquid. Solidification of this interstitial liquid takes much longer then the rapid growth of the backbone segment. After a period of time without any interstitial solidification, a new backbone-like segments of the peritectic [β] phase occurs.

The amount of the interstitial liquid just before the occurrence of a peritectic segment is estimated to be only 17% rather than the expected 34%.A comparison of the segment's width with that of the original interstitial liquid shows no increase in size.Thus, the expected transformation from the primary to the peritectic phase does not takes place.

In order to analyze the growth temperature of both the cellular growing primary [α] phase and the unsteady segment growth of the peritectic [β] phase, we have estimated the corresponding tip temperatures from the position in the sample. Knowing that the flat s/l interface at rest positioned itself at the liquidus temperature, the constant temperature gradient can be used to correlate position and temperature. Fig. 7 shows that the [α] cell tips start growing with a tip temperature of $T_\alpha$ = 413.1 K(that's $\Delta T_\alpha$ = 0.5 K below [α] phase liquidus) and then gradually decrease to $T_\alpha$ = 409.4 K after 12 hours. As already discussed in a former publication of the authors [?] the retreat of the cell tip position is caused by an increasing concentration in bulk melt. This so-called macrosegregation is originated by the convection pattern mentioned in the next section. Assuming that the growth undercooling of the cell tips does not change much with concentration, the decrease of the tip temperature can be used to estimate that the bulk concentration has changed from $x$ = 0.49 to $x$ = 0.56. Fig. 8 has been used to demonstrate the evolution of the cell tip temperature during the course of the experiment overlaid to the phase diagram.

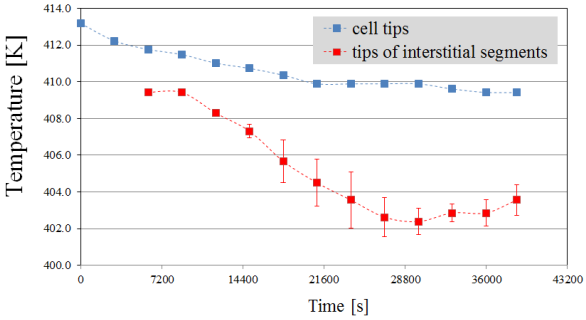


Fig. 7: Temperature level at the cell tips and the tips of interstitial segments

Fig. 7 also shows that the backbone-like [β] segments in the interstitial liquid start growing with a tip temperature of $T_\beta$ = 409.5 K (that's $\Delta T_\beta$ = 2 K below the metastable [β] phase liquidus) and then gradually decrease to around $T_\alpha$ = 402.4 K after 8 hours. As this growth is irregular the corresponding tip temperature reveals a relatively large error bar. Again assuming that the growth undercooling does not change much with concentration, the decrease of its tip temperature shows that the interstitial concentration increases from $x$ = 0.52 to $x$ = 0.77. In Fig. 8 this is indicated by the red line parallel to the [β] phase liquidus.

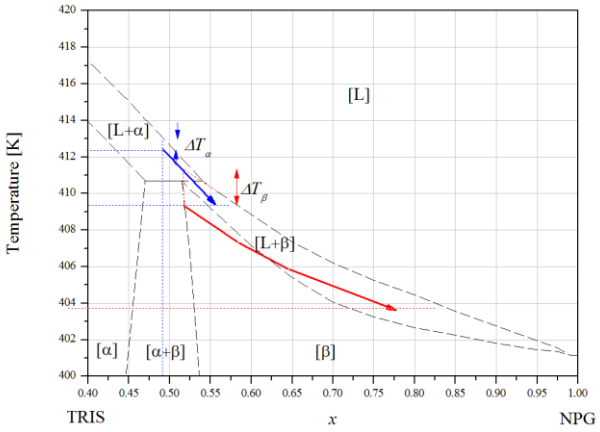


Fig. 8: Variation of tips temperature and alloy concentration for the primary[α] (blue) and the peritectic [β] phase (red).

### *B. Solidification progression*

At the beginning of the solidification experiment, which is presented in Fig. 9, the [α]phase grows with a planar interface while rejecting constantly solute into the liquid. As a NPG enriched liquid is lighter, buoyancy leads to the formation of

two counter-rotating vortices with rising liquid on the right and left wall of the sample. As consequence, the concentration ahead of the s/l interface is not uniform and the planar solidification front becomes convex with a higher NPG concentration at the right and left wall. Furthermore, the curved s/l interface reveals small perturbations which further develop into shallow cells. Simultaneously, the [β] phase nucleates close to the sample side wall and spreads perpendicularly to the sample axis. Obviously, the corresponding bandsinteract with the intercellular liquid of the [α] cells where new phase boundaries form (Fig. 9a). This observation suggests that the [β]phase grows between the (front and back)glass wallsand the primary phase.

The [β] phase never completely engulfs the [α] phase. Instead, both phases grow in a competing manner, initiating peritectic coupled growth (Fig. 9b). Such eutectic like peritectic solidification structure is described for the model system TRIS-NPG in more details in [32, 34]. However, this solidification morphology does not remain stable. First, the primary phase grows slightly faster than the peritectic phase. This is optically recognizable as the distance between the cells of the [α] phase and the [β] phase gradually increases. Furthermore, the growth morphology of the [α] phase transforms from shallow to deep cells and the [β] phase growth becomes more finger-like along the vicinity of the interstitial liquid of the [α] deep cells. While the distance between the two phases increase, also irregular backbone-like segment growth within the interstitial liquid of the [α] deep cells occur.

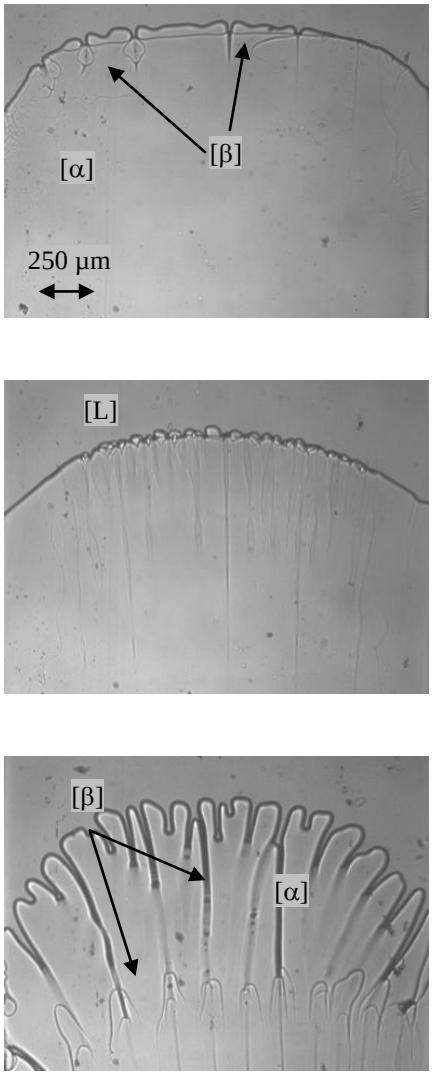


Fig. 9: Solidification progression for $x$ = 0.49.

The corresponding tip temperatures calculated from the position is shown graphically in Fig. 10.

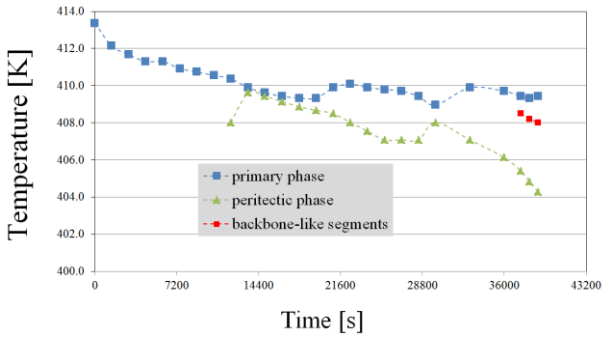


Fig. 10: Calculated temperature for the curved s/l interface (blue), the interface of the β phase after nucleation (green), and the tip of the backbone-like segments in the interstitial liquid (red).

The corresponding interpretation of the concentration distribution is given in Figure Fig. 11.The concentration in the interstitial liquid where the backbone-like segments grow reaches a value of $x$ = 0.75; this is a similar valueas for the previous experiment.

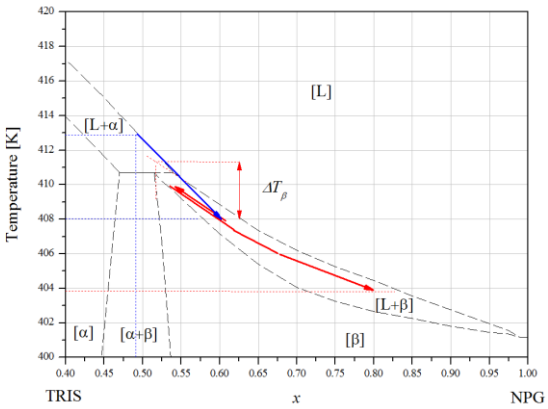


Fig. 11: Concentration distribution ahead of the s/l interface.

### *C. Planarsolidification morphology*

In the resting sample, a s/l interface and a s/s interface can be seen, like for the hypo-peritectic concentrations as described before. At the beginning of the experiment, the planar interface tries to approach the temperature level of the solidus line. After about 5400 s, the formation of small inclusions within the solid just below the s/l interface can be observed, as shown in Fig. 12. Since an s/l interface and an s/s interface existed at the beginning of the experiment, the initial phase can be assumed as the primary α phase, according to the phase diagram. The observation of the first inclusions occurs at a temperature level of 409 K, as in the two experiments described above. Thus, the inclusions consist of the β phase (Fig. 13).

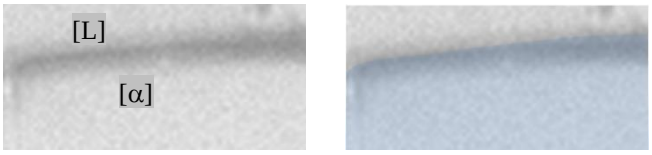


(a) $t$ = 9300 s

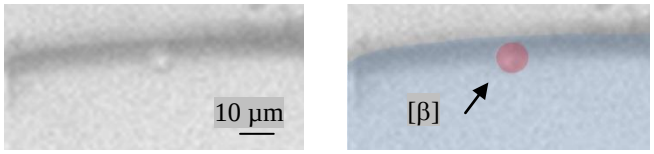


(b) $\Delta t$ = 30 s

Fig. 12: Solidification morphologies for $x$ = 0.53.

This suggests that the required undercooling for the peritectic phase, necessary for stable growth, is approximately 1.5 K below the peritectic temperature.

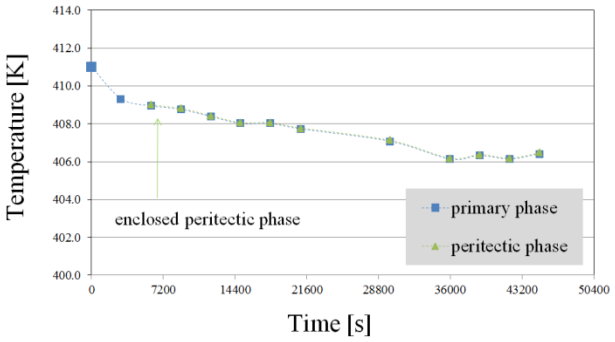


Fig. 13: Determination of the temperature level.

Fig. 14 displays the interpretation of the concentration distribution ahead of the solidification front for both phases.

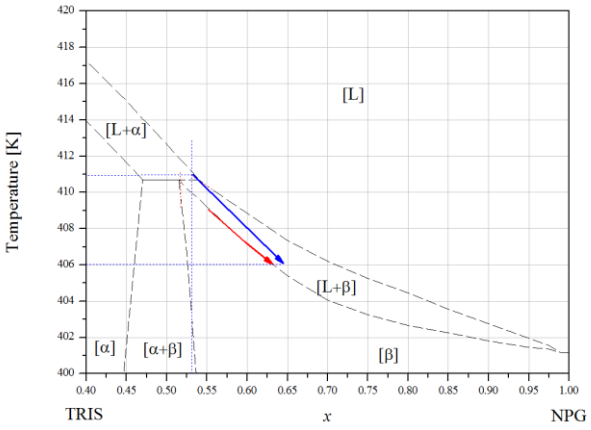


Fig. 14: Concentration distribution.

## CONCLUSIONS

The organic substances TRIS and NPG were used as a model system for peritectic solidification morphologies. The dynamics of the s/l interface were investigated under conditions where (i) both phases solidify cellular/dendritically, (ii) close to the critical velocity and (iii) under conditions where both phases solidify in a planar manner.

(i) For cellular/dendritic growth conditions, observations indicate that the primary α phase grow continuously in a cellular/dendritic pattern, as expected. In contrast, the peritectic β phase solidified dendritically and discontinuously within the intercellular/dendritic liquid.

(ii) Close to the critical velocity, the formation of a peritectic band was observed. This band enveloped the existing primary phase, consequently leading to peritectic coupled growth. However, this morphology was unstable and finally, only the primary phase grew stably in the form of deep cells.

(iii) For a planar solidification front, multiple nucleation of the peritectic phase at the s/l interface of the α phase could be detected. Whereby, the growing β phase would become immediately enclosed in a spherical form within the primary phase.

### *Acknowledgement*

This research has been supported by the Austrian Research Promotion Agency (FFG),within the framework of the MET-TRANS –ISS Space projects and by the European Space Agency (ESA) as a part of the METCOMP project.

### *References*

[1] Boettinger, W.J.(1974)The structure of directionally solidified two-phase Sn-Cd peritectic alloys. Metall. Trans., 5, 2023–2031.

[2] Trivedi, R. (1995) Theory of layered-structure formation in peritectic systems. Metall Mater Trans., 26(6), 1583-1590.

[3] Uhlmann, D.R., Chadwick, G.A. (1961) Unidirectional solidification of melts producing the peritectic reaction. Acta Metall., 9, 835–840.

[4] Trivedi, R, Park, J. (2002)Dynamics of microstructure formation in the two-phase region of peritectic systems. J. Cryst. Growth, 235, 572–588.

[5] Trivedi, R., Shin, J.H. (2005)Modelling of microstructure evolution in peritectic systems. Mater. Sci. Eng. A, 413–414 288–295.

[6] Yasuda, H., Notake, N., Tokieda, K., Ohnaka, I. (2000)*In-situ* observation of peritectic solidification in Sn-Cd and Fe-C alloys. J. Cryst. Growth, 210, 637–645.

[7] Kohler, F., Germond, L., Wagnière, J.D., Rappaz, M. (2000)Isothermal Peritectic Coupled Growth in Directionally Solidified Cu-20 wt. pct. Sn Alloy. Acta Mater., 57, 56-68.

[8] Karma, A., Rappel, W. J., Fuh, B. C., Trivedi, R.(1998)Model of banding in diffusive and convective regimes during directional solidification of peritectic systems. Metall. Trans., A 29, 1457–1470.

[9] Tokieda, K., Yasuda, H., Ohnaka, I.(1999)Formation of banded structure in Pb-Bi peritectic alloys. Mater. Sci. Eng., A 262, 238–245.

[10] Lograsso, T. A., Fuh, B. C., Trivedi, R.(2005)Phase selection during directional solidification of peritectic alloys. Metall. Trans., A 36, 1287–1300.

[11] Liu, S., Trivedi, R.(2006)Effect of thermosolutal convection on microstructure formation in the Pb-Bi peritectic system. Metall. Trans., A 37, 3293–3304.

[12] Ma, D., Li, Y., Ng, S.C., Jones, H.(2000)Unidirectional solidification of Zn-rich Zn–Cu peritectic alloys—I. Microstructure selection Acta Mater., 48, 419–431.

[13] Ma, D., Li, Y., Ng, S.C., Jones, H.(2000)Unidirectional solidification of Zn-rich Zn–Cu peritectic alloys—II. Microstructural length scales. Acta Mater., 48, 1741–1751.

[14] Titchener AP, Spittle JA, 1975 The microstructures of directionally solidified alloys that undergo a peritectic transformation. Acta Metall. , 3, 497–502.

[15] Busse, P., Meissen, F. (1997)Coupled growth of the properitectic α- and the peritectic γ-phases in binary titanium aluminides. Scripta Mater., 36, 653–658.

[16] Luo, L.S., Su, Y.Q., Guo ,J.J., Li, X.Z., Li, S.M., Zhong, H., Liu, L., Fu, H.Z.(2008)Peritectic reaction and its influences on the microstructures evolution during directional solidification of Fe–Ni alloys. J. Alloys Comp., 461, 121–127.

[17] Vandyoussefi, M., Kerr, H.W., Kurz, W. (2000)Two-phase growth in peritectic Fe–Ni alloys. Acta Mater., 48,

2297–2306.
[18] Lo, T.S., Dobler, S., Plapp, M., Karma, A., Kurz, W.(2003) Two-phase microstructure selection in peritectic solidification: from island banding to coupled growth. Acta Mater., 51, 599-611.
[19] Dobler, S., Lo, T.S., Plapp, M., Karma, A., Kurz, W. (2004) Peritectic coupled growth. Acta Mater., 52, 2795–2808.
[20] Vandyoussefi, M., Kerr, H.W., Kurz, W.(1997)Directional solidification and δ/γ solid state transformation in Fe 3% Ni alloy. Acta Mater., 45, 4093-4105.
[21] Lee, J.H., Verhoeven, J.D. (1994) Peritectic formation in the Ni-Al system. J. Cryst. Growth, 144, 353–366.
[22] Zhong, H., Li, S.M., Lü, H.Y., Liu, L., Zou, G.R., Fu, H.Z. (2008) Microstructure evolution of peritectic Nd14Fe79B7 alloy during directional solidification. J. Cryst. Growth, 310, 3366–3371.
[23] Barrio, M., Lopez, D.O., Tamarit, J.L., Negrier, P., Haget, Y. (1995) J. Mater. Chem., 5, 431-437.
[24] Mogeritsch, J., Ludwig, A., Eck, S., Grasser, M., McKay, B. (2009)Stability investigations of a binary organic alloy system with a peritectic phase diagram. Scripta Mater., 60, 882-885
[25] Mogeritsch, J., Eck, S., Grasser, M., Ludwig, A. (2009)In situ observation of solidification in an organic peritectic alloy system. Mater. Sci. Forum, 649, 159-64
[26] Ludwig, A., Mogeritsch, J., Grasser, M.(2009)In-situ observation of unsteady peritectic growth modes. Trans. Indian Inst. Metals, 62, 433-436
[27] Mogeritsch, J. (2011)Investigation on peritectic solidification using a transparent organic system. Ph.D. Thesis, University of Leoben
[28] Ludwig, A, Mogeritsch, J. (2011) In-situ observation of coupled peritectic growth. In: Solidif Sci Technol Proc John Hunt Int Symp, pp. 233-242.
[29] Mogeritsch, J,, Ludwig, A. (2011) In-situ observation of coupled growth morphologies in organic peritectics. IOP Conf Ser Mater Sci Eng 7: 12028.
[30] Mogeritsch, J., Ludwig, A. (2012) Microstructure formation in the two phase region of the binary peritectic organic system TRIS-NPG. In: TMS Annual Meeting Symposium, Materials Res Microgravity, Orlando, Florida, USA, 48-56.
[31] Ludwig, A., Mogeritsch, J. (2014) Recurring instability of cellular growth in a near peritectic transparent NPG-TRIS alloy system. Mater Sci Forum, 317-322.
[32] Mogeritsch J, Ludwig A (2015) In-situ observation of the dynamic of peritectic coupled growth using the binary organic system TRIS-NPG. IOP Conf Ser Mater Sci Eng., 84, 12055.
[33] Ludwig A, Mogeritsch J. (2016) Compact seaweed growth of peritectic phase on confined, flat pro-peritectic dendrites. Journal of Crystal Growth, 455, 99-104.
[34] Ludwig, A., Mogeritsch, J., Pfeifer, T. (2017) In-situ observation of coupled peritectic growth in a binary organic model alloy. Acta Mat. 126, 329-335.
[35] Mogeritsch, J. P., Ludwig, A. (2018) Investigation on peritectic layered structures by using the binary organic components TRIS-NPG as model substances for metal-like solidification, Crimson Publishers, Res Dev Mater Sci 4(1) 1-3.
[36] Mogeritsch, J. P., Pfeiler, T., Ludwig, A. (2018) Investigation on the liquid flow ahead of the solidification front during the formation of peritectic layered solidification structure, 7th International Conference on Solidification and Gravity, University of Miskolc 319-324.
[37] Mogeritsch, J. P., Ludwig, A. (2018) Investigation on the binary organic components TRIS-NPG as suitable model substances for metal-like solidification. 7th International Conference on Solidification and Gravity, University of Miskolc 330-335.